Behavioural Brain Research 210 (2010) 155–163

Contents lists available at ScienceDirect

Behavioural Brain Research

journal homepage: www.elsevier.com/locate/bbr

Research report

# Dopaminergic dysregulation in mice selectively bred for excessive exercise or obesity

Wendy Foulds Mathes[b,*,1], Derrick L. Nehrenberg[a,1], Ryan Gordon[a], Kunjie Hua[b], Theodore Garland Jr.[d], Daniel Pomp[a,b,c,2]

[a] Department of Nutrition, University of North Carolina at Chapel Hill, 120 Mason Farm Rd, CB#7264, Chapel Hill, NC 27599-7264, USA
[b] Department of Genetics, University of North Carolina at Chapel Hill, 120 Mason Farm Rd, CB #7264, Chapel Hill, NC 27599-7264, USA
[c] Department of Cell and Molecular Physiology, University of North Carolina at Chapel Hill, 120 Mason Farm Rd, CB#7264, Chapel Hill, NC 27599-7264, USA
[d] Department of Biology, 109 University Lab Building, University of California at Riverside, Riverside, CA 92521, USA

ARTICLE INFO

*Article history:*
Received 17 October 2009
Received in revised form 4 February 2010
Accepted 7 February 2010
Available online 13 February 2010

*Keywords:*
Monoamines
Body weight
Physical activity
Microarray
Nucleus accumbens
Dorsal striatum
Gene expression

ABSTRACT

Dysregulation of the dopamine system is linked to various aberrant behaviors, including addiction, compulsive exercise, and hyperphagia leading to obesity. The goal of the present experiments was to determine how dopamine contributes to the expression of opposing phenotypes, excessive exercise and obesity. We hypothesized that similar alterations in dopamine and dopamine-related gene expression may underly obesity and excessive exercise, as competing traits for central reward pathways. Moreover, we hypothesized that selective breeding for high levels of exercise or obesity may have influenced genetic variation controlling these pathways, manifesting as opposing complex traits. Dopamine, dopamine-related peptide concentrations, and gene expression were evaluated in dorsal striatum (DS) and nucleus accumbens (NA) of mice from lines selectively bred for high rates of wheel running (HR) or obesity (M16), and the non-selected ICR strain from which these lines were derived. HPLC analysis showed significantly greater neurotransmitter concentrations in DS and NA of HR mice compared to M16 and ICR. Microarray analysis showed significant gene expression differences between HR and M16 compared to ICR in both brain areas, with changes revealed throughout the dopamine pathway including D1 and D2 receptors, associated G-proteins (e.g., *Golf*), and adenylate cyclase (e.g., *Adcy5*). The results suggest that similar modifications within the dopamine system may contribute to the expression of opposite phenotypes in mice, demonstrating that alterations within central reward pathways can contribute to both obesity and excessive exercise.



## 1. Introduction

Within the central nervous system, neurotransmitters, peptides, and hormones interact to establish a balance between energy intake and energy expenditure, resulting in body weight regulation and homeostasis. Dopamine plays a key role in this complex system, modulating such motivated behaviors as food intake and physical activity. Moreover, disruption of normative neurotransmission within dopaminergic pathways has been implicated in binge eating, obesity, and hyperactivity [1–7]. The genetic underpinnings of such behaviors are not well understood.

Running-wheel activity has been shown to be rewarding and as such a motivated behavior. For instance, rats can be conditioned to lever press for access to running wheels [8–10]. Similarly, rats trained to associate a novel environment with the after-effects of wheel running choose to spend more time in that environment compared to an environment not paired with wheel running [11]. Interestingly, mice selectively bred for high rates of wheel running (HR) show decreased operant responding for short periods of wheel access compared with control mice; but when trained to respond for longer periods of access, rates of responding do not differ among HR and control lines [12]. These data suggest that HR mice may have an altered reward threshold for wheel running compared to controls. As such, it is possible that HR mice need to run longer, at a higher intensity, to get the same reward from wheel running that control mice receive after shorter, less intense bouts. If true, this would imply that the endogenous reward system in HR mice is dysregulated. In fact, data from pharmacological experiments suggest that dopamine function in HR mice is altered [13,14]. For instance, psychostimulants such as methylphenidate (Ritalin) and cocaine, that stimulate locomotor behavior and wheel run-

* Corresponding author at: Department of Genetics, University of North Carolina at Chapel Hill, 120 Mason Farm Rd, CB #7264, Chapel Hill, NC 27599-7264, USA. Tel.: +1 919 966 0091; fax: +1 919 843 4682.
*E-mail addresses:* wfmathes@med.unc.edu (W.F. Mathes), dpomp@unc.edu (D. Pomp).
[1] These authors contributed equally to this work.
[2] Tel.: +1 919 966 0013; fax: +1 919 843 4682.

0166-4328/$ – see front matter © 2010 Elsevier B.V. All rights reserved.
doi:10.1016/j.bbr.2010.02.016

ning in control mice, decrease wheel running in HR mice. Similarly, dopamine receptor antagonists that decrease locomotor behavior in control mice have reduced efficacy or are ineffective in altering wheel running in HR mice [13,14]. It is hypothesized that the dopamine dysregulation in HR mice manifests as either decreased DA concentrations, decreased DA receptor densities, or reduced second-messenger signaling [15].

Dopamine dysregulation has also been postulated to contribute to development of obesity and binge eating. Data have illustrated that alterations in the D2 dopamine receptor are linked to increased reward sensitivity in obese and binge eating individuals [3]. Likewise, research examining obesity-prone rats revealed dopamine deficiencies in the nucleus accumbens and dorsal striatum that were directly linked to hyperphagia and increased body mass [5]. Dopamine D4 receptors are associated with binge eating in depressed individuals and individuals with bulimia nervosa [16,17]. In addition, dopamine transporter knock-down mice that show chronically elevated tissue dopamine display increased goal-directed behavior for food reward [18].

Taken together, dopaminergic dysregulation is associated with the expression of both physical activity and obesity-related phenotypes. The mode of this dysregulation has yet to be fully elucidated. The *dual vulnerability* theory of dopamine dysregulation presents two opposing hypotheses as to how dopamine and reward sensitivity may contribute to the expression of motivated behaviors, such as food intake and exercise [3]. The first hypothesis, Reward Deficiency Syndrome, states that individuals with low dopaminergic function seek rewarding substances (e.g., food, drugs of abuse) to increase endogenous dopamine levels and improve mood [19]. Alternatively, hyper-sensitivity to reward paired with increased dopaminergic functioning may motivate an individual to seek rewarding stimuli simply because the reinforcement value of the reward is so great [3].

The aim of the current research was to examine neuropeptide and gene expression in midbrain dopaminergic nuclei of mice with genetically predisposed extreme physical activity and obesity phenotypes. In addition, the effect of wheel running on brain dopamine concentrations and gene expression was evaluated in these mice. Mice having undergone long-term selective breeding for high rates of wheel running (HR) or increased body mass and body fat (M16) were used as representative models for extreme and dichotomous behavioral phenotypes. HR mice, selected for high rates of wheel running on days 5 and 6 of a 6-day wheel exposure from an ICR (Institute of Cancer Research) background strain, run significantly more, faster, and are significantly leaner than non-selected ICR controls [20–22]. M16 mice, also selected from the ICR strain, are heavier, hyperphagic, and have significantly greater amounts of body fat than ICR controls [21,23]. We hypothesize that similar modifications in dopamine signaling and dopamine-related gene expression may contribute to the expression of opposite phenotypes in mice, suggesting that alterations within central reward pathways can contribute to both obesity and excess physical activity.

## 2. Materials and methods

### 2.1. Animals

Male and female mice (8 weeks of age) from three different strains (HR, M16, ICR [21,22]) were housed individually in standard laboratory cages with attached running wheels (1.12 m diameter, Lafayette Industries, Lafayette, IN) in a temperature (23 ± 1 °C) and humidity controlled vivarium with a standard 12/12 light dark cycle (lights on 0700 h). One-half of the animals in each strain and sex ($N$ = 10–12) were allowed free access to the wheels for 6 days, while access to the wheels was blocked for the remaining half ($N$ = 10–12). All mice had *ad libitum* access to standard laboratory chow (LabDiet 5053, TestDiet, Richmond, IN) and water. Body weight and composition were measured immediately prior to the start of the experiment and again after the 6-day wheel trial. Body composition was assessed using MRI (EchoMRI, Houston, TX) to determine fat and lean mass percentages. Food was weighed prior to the start of the experiment and again after 6 days. Daily average food intake was calculated by dividing the total amount of food eaten during the experiment by the number of days (i.e. 6). Wheel running was recorded continuously over the 6-day period using an automated activity wheel monitoring program (AWM, Lafayette Industries, Lafayette, IN).

After body composition measurements on day 6, mice were sacrificed by cervical dislocation and whole brains were immediately removed and placed in 0.9% saline chilled to 4 °C for 30 s to firm the tissue. Chilled brains were placed on an aluminum block chilled on ice. A 1.0 mm coronal slice was taken between Bregma 1.70 and 0.74 mm [24]. Brains were placed posterior side up and a horizontal cut was made beneath the lateral ventricle to produce a horizontal section containing the nucleus accumbens. Another horizontal cut was made beneath the corpus callosum to produce a section containing the caudate putamen (here forth referred to as dorsal striatum). Cerebral cortex was removed from the edges of these sections. Ventral pallidum was then removed from the nucleus accumbens section. Finally, both sections were bisected at the midline to produce left and right hemisphere tissues of caudate putamen and nucleus accumbens. Freshly dissected tissues were flash frozen in liquid nitrogen and stored at −80° C. Samples to be used for gene expression studies were placed in RNA*later* (Ambion/Applied Biosystems, Austin, TX) prior to freezing.

### 2.2. Brain monoamines

Nucleus accumbens and dorsal striatum tissue samples were weighed and transferred to a contract service provider (Dr. Richard Mailman, Department of Psychiatry, NC Neurosciences Hospital) where norepinephrine (NE), dopamine (DA), the dopamine metabolites 3,4-dihydroxyphenylacetic acid (DOPAC) and homovanillic acid (HVA), serotonin (5HT), and its metabolite 5-hydroxyindoleacetic acid (5HIAA) concentrations were analyzed using high performance liquid chromatography (HPLC)-electrochemical detection methods as described elsewhere [25,26]. Serotonin levels were not reported for the nucleus accumbens samples because concentrations were too low to be reliably detected. Concentrations of monoamines and their metabolites within each sample were calculated in reference to established standard curves. Data were expressed as nanogram of compound per milligram of brain tissue. The ratio of individual metabolites to monoamine concentrations was calculated as an indirect measure of monoamine turnover.

### 2.3. RNA isolation and purification

RNA was isolated from thawed tissue samples using the Qiagen RNeasy Lipid Tissue Mini Kit (Qiagen Inc., Valencia, CA) according to the manufacturer's protocol. Briefly, samples were placed into 1 ml of QIAzol lysis reagent and the lysate homogenized using a tissue homogenizer. RNA was separated from the homogenate using chloroform, mixed with 70% ethanol and transferred to a binding column. RNA was rinsed using a series of buffer solutions and eluted with distilled $H_2O$. RNA quality and quantity was determined by full spectrum spectrophotometry (NanoDrop ND-1000, NanoDrop Technologies, Wilmington, DE) and bio-analysis (Genomics and Bioinformatics Core Facility, Lineberger Comprehensive Cancer Center, UNC School of Medicine, Chapel Hill, NC). Any sample with a 260/230 ratio lower than 1.8 was purified using sodium acetate precipitation and re-evaluated for quantity and quality.

### 2.4. Gene expression analysis

Approximately 300 ng RNA was amplified and biotin labeled using Illumina TotalPrep RNA Amplification Kit (Ambion/Applied Biosystems, Austin, TX) according to the manufacturer's protocol. cRNA was eluted with warm, nuclease-free water and quantified using spectrophotometry. A total of 1.5 μg labeled cRNA was hybridized at 58 °C for 17.5 h to the Illumina Sentrix Bead Chip Array mouse 6v1.1 (Illumina, San Diego, CA) according to the manufacturer's protocol. Arrays were washed, blocked, and analyzed using Illumina BeadArray reader (Mammalian Genotyping Core, Lineberger Comprehensive Cancer Center, UNC School of Medicine, Chapel Hill, NC). Image files were extracted using Illumina Bead Studio v3.0.

### 2.5. Statistical analysis

Main effects of strain, sex, running condition (wheel access or not), and the interactions among the three on body weight, body composition, food intake, and brain monoamine concentrations were determined using multivariate GLM ANOVA (SPSS, Chicago, IL). A separate multivariate GLM ANOVA was performed to identify significant effects of strain and sex on wheel running distance and speed, with wheel freeness as a covariate. LSD and multiple $t$-test post hoc analyses were used to delineate significant main effects of strain and sex, respectively.

Using a hypothesis-driven approach (e.g., see Bronikowski et al. [57]), 129 genes were chosen *a priori* using Ingenuity Pathway Analysis (IPA, Ingenuity Systems, Redwood City, CA, USA) and citations from the literature for their role in the dopamine signaling pathway, G-protein coupled receptor mediated signaling, as well as common neurotransmitters known to interact with the dopamine system within the two brain areas examined (Supplemental material) Gene expression differences were determined using the SAM statistical package for microarray analysis (Stanford University, Palo Alto, CA). Raw gene expression scores were exported from Bead Studio and normalized using Loess-Quantile normalization methods using R v2.9.0

statistical software (www.r-project.com). Transcripts with a detection score greater than or equal to 0.95 were imported into SAM for differential expression analysis. Significant expression differences were detected using the two class unpaired *t*-statistic and 1000 permutations. Genes detected with a FDR <0.01% and displaying fold changes greater than 1.5 were considered significant. Using both FDR and fold change to determine significant differences in gene expression increases the reproducibility of the results as well as the likelihood that differences in gene expression detected in the analyses have biological relevance [27,28].

## 3. Results

### 3.1. Body weight and composition prior to wheel running

Prior to the initiation of the 6-day wheel trial, there were significant strain differences in body weight ($p < 0.001$), percent lean mass ($p < 0.001$), and percent fat mass ($p < 0.001$ (Table 1). M16 mice had higher values than HR mice, with ICR being intermediate, for each phenotype. Likewise, there were significant effects of sex on body weight ($p < 0.001$) and percent lean mass ($p < 0.001$), with males having increased values, and significant sex by strain interactions for body weight ($p < 0.002$), percent lean mass ($p < 0.001$), and percent fat mass ($p < 0.002$, Table 1). There was no statistical difference in percent body fat between males and females in the HR and ICR strains; however, female M16 mice had significantly greater body fat percentages than their male counterparts ($p < 0.02$) (Table 1).

### 3.2. Wheel running

Significant strain differences were also identified in wheel running behavior. Multivariate GLM ANOVA revealed significant strain differences in total distance run ($p < 0.001$) and average running speed ($p < 0.001$), a significant effect of sex ($p < 0.005$) and a sex by strain interaction ($p < 0.05$) in total distance run on days 5 and 6 of the experiment (Table 2). LSD and multiple *t*-test post hoc tests showed that the HR mice ran significantly greater distances ($p < 0.001$) and at faster speeds ($p < 0.001$) than either the ICR or M16 mice (Fig. 1). There were no differences in running distance or speed between males and females within the HR or M16 strains. However, within the ICR strain, males ran significantly less than the females ($p < 0.03$) (Fig. 1).

As expected, running-wheel activity had profound effects on body composition and food intake. Details of the effects of wheel running on body composition and food intake in these mouse strains have been recently described by Nehrenberg et al. [29]. Because the effects of wheel running in this experiment are consistent with previous findings, and the focus of this manuscript is on the strain differences and wheel running in dopamine-related functions in the CNS, data regarding wheel running effects on body composition are not presented or discussed.

### 3.3. Brain monoamines

Analysis of neurochemical concentrations within the dorsal striatum and nucleus accumbens of male and female HR, ICR, and M16 mice showed significant strain effects on monoamine concentrations. Specifically, analyses revealed significant effects of strain on the concentration of dopamine ($p < 0.001$), the dopamine metabolites DOPAC ($p < 0.01$) and HVA ($p < 0.001$), and nore-

**Table 1**
Body weight and body composition of HR, M16 and ICR mouse strains prior to wheel running.

| | | Body weight (g) | Lean mass (%) | Fat mass (%) |
|---|---|---|---|---|
| HR | Females | 23.79 ± 2.22[b,d] | 85.49 + 2.43[b,d] | 10.17 ± 2.26[b,d] |
| | Males | 29.5 ± 3.46[b,d,*] | 83.42 + 2.41[b,d,*] | 10.01 ± 2.14[b,c] |
| ICR | Females | 28.83 ± 2.51[b,f] | 77.03 ± 4.02[b,f] | 17.04 ± 3.98[b,f] |
| | Males | 35.98 ± 3.81[b,f,*] | 78.12 ± 3.60[a,f,*] | 14.03 ± 3.97[b,d] |
| M16 | Females | 45.6 ± 5.84[d,f] | 66.60 ± 4.52[d,f] | 28.85 + 4.44[d,f,*] |
| | Males | 42.23 ± 2.79[d,f,*] | 74.30 ± 5.63[c,f,*] | 19.45 ± 5.63[d,f] |

Data expressed as mean ± SEM.
[a] Significantly different than M16, $p<0.05$.
[b] $p<0.01$.
[c] Significantly different than ICR, $p<0.05$.
[d] $p<0.01$.
[e] Significantly different than HR, $p<0.05$.
[f] $p<0.01$.
[*] Significant differences between males and females, $p<0.05$.

**Table 2**
Correlations among monoamine concentrations and wheel running in the nucleus accumbens of HR, M16 and ICR mice.

| | | Average speed | | | Average distance | | |
|---|---|---|---|---|---|---|---|
| | | HR | M16 | ICR | HR | M16 | ICR |
| Dopamine | Pearson correlation | −0.36 | 0.14 | 0.06 | −0.37 | 0.08 | 0.04 |
| | Sig. (2-tailed) | *0.03 | 0.40 | 0.74 | *0.03 | 0.63 | 0.80 |
| | *N* | 34 | 40 | 36 | 34 | 40 | 36 |
| Norepinephrine | Pearson correlation | −0.28 | −0.05 | −0.02 | −0.25 | 0.07 | 0.00 |
| | Sig. [2-tailed) | 0.10 | 0.78 | 0.89 | 0.15 | 0.65 | 1.00 |
| | *N* | 35 | 41 | 36 | 35 | 41 | 36 |
| DOPAC | Pearson correlation | −0.41 | −0.08 | _0.04 | −0.43 | −0.14 | −0.02 |
| | Sig. (2-tailed) | *0.01 | 0.60 | 0.82 | *0.01 | 0.37 | 0.90 |
| | *N* | 35 | 41 | 36 | 35 | 41 | 36 |
| HVA | Pearson correlation | −0.36 | −0.16 | 0.20 | −0.36 | −0.18 | 0.21 |
| | Sig. (2-tailed) | *0.03 | 0.33 | 0.24 | *0.03 | 0.25 | 0.22 |
| | *N* | 35 | 41 | 36 | 35 | 41 | 36 |
| 5HIAA | Pearson correlation | −0.32 | −0.12 | −0.18 | −0.33 | −0.12 | −0.15 |
| | Sig. (2-tailed) | 0.06 | 0.46 | 0.30 | 0.06 | 0.44 | 0.39 |
| | *N* | 35 | 41 | 36 | 35 | 41 | 36 |

[*] $p < 0.05$.

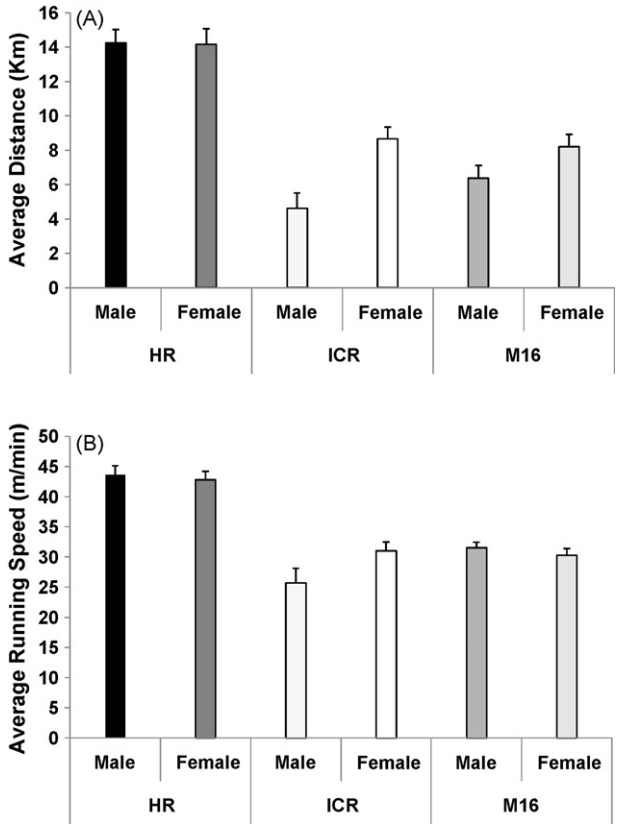


**Fig. 1.** Wheel running distances (A) and running speed (B) in HR, M16 and ICR mice. Mice were given access to running wheels for 6 days and distances and speeds for days 5 and 6 were averaged. HR mice ran significantly greater distances ($F(2,60) = 56.82$, $p < 0.001$) at greater speeds ($F(2,60) = 54.37$, $p < 0.001$) than M16 and ICR mice. There were no differences in running distance or speed between males and females within the HR or M16 strains. However, within the ICR strain, males ran significantly less than the females ($t(17) = 3.68$, $p < 0.03$). Data are presented as mean ± SEM.

pinephrine ($p < 0.05$) in the nucleus accumbens (Fig. 2a). LSD post hoc comparisons revealed that monoamine and metabolite concentrations in the nucleus accumbens of HR mice were significantly greater than either the M16 or the ICR mice. Analyses also showed a significant strain by sex interaction for DA ($p < 0.01$), DOPAC ($p < 0.05$), and HVA ($p < 0.01$) concentrations (Fig. 2a). Female HR mice showed significantly higher DA concentrations in the nucleus accumbens than their male counterparts, while M16 males displayed significantly greater DA, DOPAC, and HVA concentrations than their female counterparts (Fig. 3).

Within the dorsal striatum, analyses showed significant strain effects on concentrations of dopamine ($p < 0.001$), DOPAC ($p < 0.001$), HVA ($p < 0.001$), serotonin ($p < 0.01$) and its metabolite 5HIAA ($p < 0.01$). Post hoc tests demonstrated that HR mice had significantly higher concentrations of all peptides than the other two strains (Fig. 2b). There were no significant effects of running-wheel activity on dorsal striatum monoamine concentrations; however, there was a significant effect of sex on 5HIAA concentrations ($p < 0.05$) and a significant strain by sex interaction for DOPAC concentrations ($p < 0.05$). Post hoc tests revealed that female mice had significantly higher 5HIAA concentrations than male mice across all 3 strains and that female HR mice had lower, while M16 and ICR females had higher, DOPAC concentrations (Fig. 2b).

Concentrations of dopamine and its metabolites within the nucleus accumbens were significantly correlated with wheel running distance and speed in HR mice, but not in M16 and ICR mice. Pearson's *R* correlations showed that greater wheel running speeds and distances were associated with lower nucleus accumbens dopamine, DOPAC and HVA concentrations in the HR mice (Table 2). Monoamine concentrations within the dorsal striatum were not significantly related to running-wheel behaviors in any of the three strains.

Univariate GLM analysis revealed significant strain effects for dopamine turnover in the nucleus accumbens ($p < 0.02$). Turnover ratios for HR mice and M16 mice were significantly lower than those of ICR mice, however, they did not differ from one another. There were no significant effects of wheel running, sex, or the interactions of wheel, sex and strain on turnover ratios in the nucleus accumbens. Turnover ratios for DA did not differ in the dorsal striatum.

### 3.4. Gene expression

Within the dorsal striatum, 38 genes were significantly differentially expressed between male HR and ICR mice. Of these, 18 were down-regulated and 20 were up-regulated in HR mice compared to ICR (Table 3). Gene expression profiles in M16 mice were significantly different from ICR, but the number of genes that differed was considerably lower than those seen with the HR by ICR comparisons. Only 8 genes were differentially expressed in M16 compared with ICR mice, with 4 down-regulated and 4 up-regulated (Table 4). Expression differences varied only slightly when analyzed separately by running condition. Significant genes, their functions and fold changes for all comparisons are listed in Tables 5 and 6.

Differences in gene expression within the nucleus accumbens were less pronounced than those observed in the dorsal striatum. Between the HR and ICR or M16 and ICR males, three genes were differentially expressed. When analyzed separately by running condition, differential gene expression did not change dramatically (Table 7). A separate experiment assessing gene expression differences in the nucleus accumbens among female runners within the HR, M16 and ICR strains showed similar results (Table 8).

## 4. Discussion

Our results demonstrate that mice selectively bred for high rates of wheel running or polygenic obesity show significant dopaminergic dysregulation compared with control ICR mice. HPLC analysis showed that HR mice had significantly elevated dopamine and dopamine metabolite concentrations in the dorsal striatum and nucleus accumbens compared to M16 and ICR mice. These results are independent of wheel activity as HR mice with and without access to wheels showed elevated levels of tissue dopamine compared to M16 and ICR mice. Calculated dopamine turnover was significantly lower in the nucleus accumbens of HR and M16 mice compared to ICR mice. Gene expression data demonstrate that these two selected lines have down-regulated dopamine receptor gene expression paired with significant alterations in gene expression for transcripts that regulate second-messenger signaling within the dorsal striatum. Fewer changes in gene expression were detected within the nucleus accumbens, yet there were significant increases, in both M16 and HR mice, in the expression of transcripts encoding genes that regulate dopaminergic neurogenesis and neurotransmission. Gene transcript expression was similar between runners and non-runners (mice housed with and without wheel access, respectively) within each of the three strains, although running-wheel activity altered gene transcript expression among the three strains. Collectively, these findings support the hypothesis that the expression of seemingly antithetical phenotypes – such as excessive exercise and obesity – may be the consequence of similar alterations in dopamine gene expression within central reward pathways [5,13,14,29,30]. However, we speculate that the

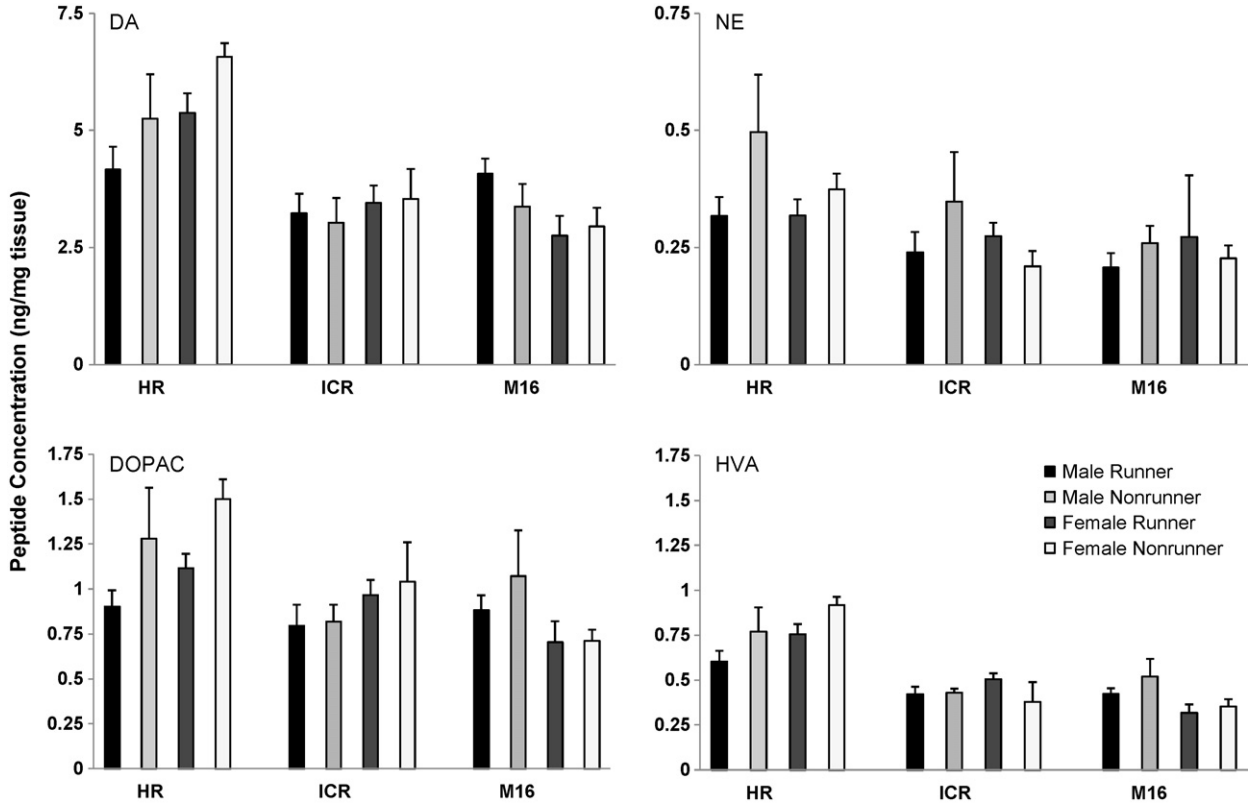


**Fig. 2.** Peptide concentrations in the nucleus accumbens for ICR, HR and M16 mice. HPLC analysis of tissue samples from nucleus accumbens in HR, M16 and ICR mice was performed to measure tissue concentrations of DA, DOPAC, HVA, NE and 5HIAA. Peptide concentrations for DA ($F(2,110) = 23.65$, $p < 0.001$), DOPAC ($F(2,110) = 8.14$, $p < 0.01$), HVA ($F(2,110) = 42.65$, $p < 0.001$) and NE ($F(2,110) = 3.44$, $p < 0.05$) were significantly higher in HR mice than in M16 or ICR mice. There were no differences in 5HIAA concentrations among the strains. DA concentrations were significantly higher in female compared to male HR mice ($F(2,110) = 5.26$, $p < 0.01$). DA ($F(2,110) = 5.26$, $p < 0.01$), DOPAC ($F(2,110) = 4.35$, $p < 0.05$) and HVA ($F(2,110) = 7.53$, $p < 0.01$) concentrations were significantly higher in male compared to female M16 mice. Data are presented as mean ± SEM.

functional consequences of these gene expression changes may be modulated by strain dependent differences in neurotransmitter concentrations, thus manifesting as opposing phenotypes.

Increased dopamine neurotransmission increases locomotor activity, prolongs the duration of physical activity, and attenuates the development of fatigue from physical activity [31,32]. Animals genetically modified to over-express dopamine, such as dopamine transporter knockout mice, also show increased locomotor activity [33]. Likewise, rats selectively bred for increased aerobic capacity show increased striatal DA activity, decreased body mass, and increased running distances compared to rats selectively bred for low aerobic capacity [34]. Thus, hyperdopaminergia in the HR mice may contribute to the expression of the excessive exercise phenotype.

Alternatively, physical activity has been shown to increase tissue dopamine levels as well as dopamine synthesis and metabolism [35,36]. However, no effects of wheel running on dopamine or dopamine metabolite concentrations in HR mice were revealed in this study. Moreover, previous studies reported significantly elevated home cage activity levels in HR mice denied access to running wheels compared to control mouse lines [37,38]. In addition, Rhodes et al. [13] showed that HR mice had elevated basal activity levels compared to controls when housed individually without wheel access for 48 h [13]. These data provide evidence to suggest that elevated dopamine levels in HR mice may be causal to, rather than an effect of, increased wheel running in these mice. In other words, elevated dopamine levels may have been a direct target of selection and a key driver of establishment of lines of mice genetically predisposed to increased activity levels, both in the home cage and when allowed to access to running wheels. However, replication of these results in one or more of the other HR replicate selection lines for wheel running [39] is required to differentiate actual selection response from possible effects of genetic drift.

Wheel running distance and speed were significantly negatively correlated with DA, DOPAC, and HVA concentrations in the nucleus accumbens of HR, but not M16 or ICR, mice suggesting the reinforcement potential of wheel running is decreased in these animals. In fact, HR mice show decreased operant responding for short, but not long, periods of wheel running access compared to control mice, indicating that HR mice may be less sensitive to the reinforcing properties of wheel running than controls [12]. Thus, the excessive exercise phenotype in HR mice is most likely a dopamine driven increase in general locomotor behavior rather than a reward driven behavior. It is important to note that increased variability in wheel running for the HR mice increased the statistical power to detect significant correlations with DA levels compared to M16 and ICR mice. When controlling for running levels using a treadmill test, HR mice failed to show any significant correlations between running and DA levels [15]. However, differences in the physiological response to treadmill versus wheel running may have contributed to these discrepant findings [40].

Tissue dopamine levels were not different between M16 and ICR mice. However, calculated dopamine turnover was significantly decreased in the NA of M16 mice compared to ICR. Decreased turnover indicates that dopamine may be persisting at the receptor for a longer period of time, leading to receptor down-regulation or desensitization and decreased dopamine neurotransmission in M16 mice. Deficiencies in dopamine neurotransmission within the nucleus accumbens have been associated with obesity phenotypes in rats [5,41]. Similarly, stimulation-induced dopamine signaling is

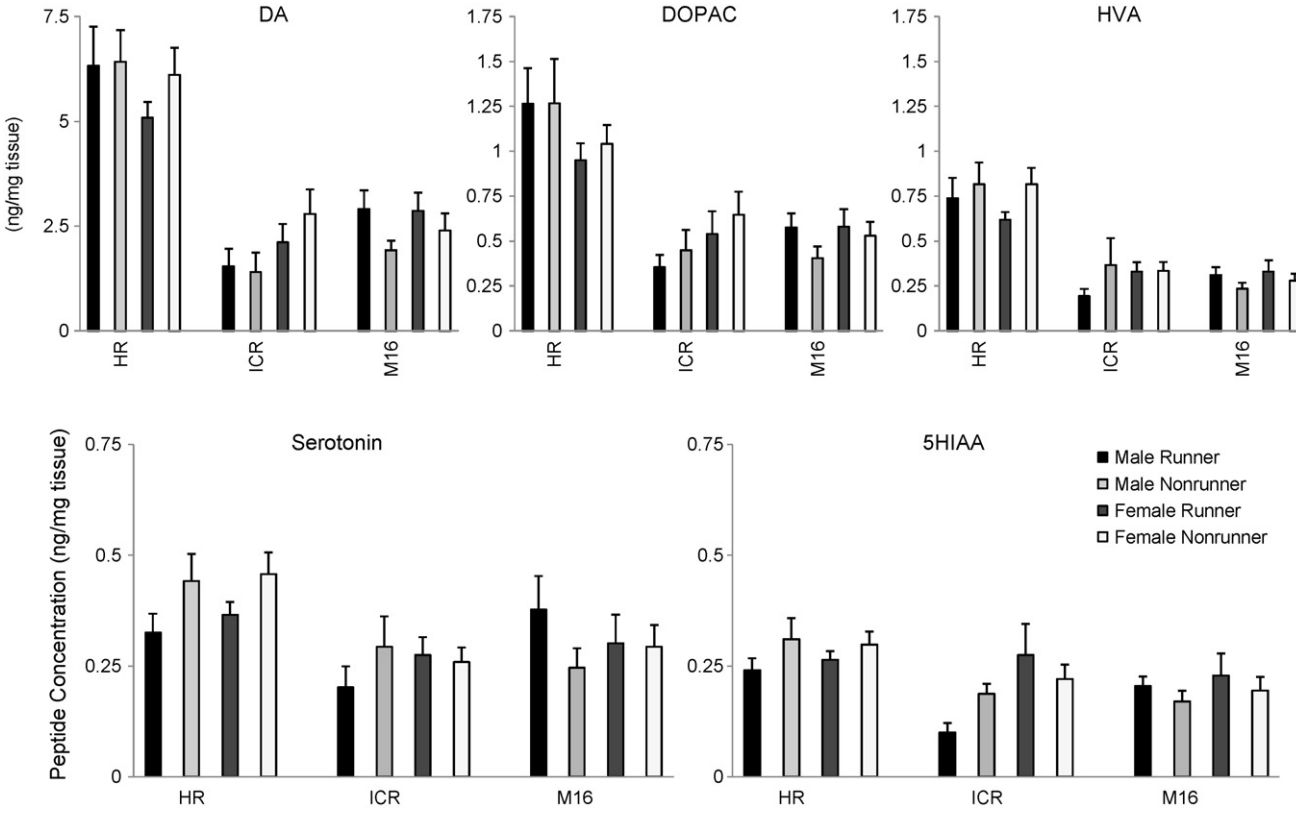


**Fig. 3.** Peptide concentrations in the dorsal striatum for ICR, HR and M16 mice. HPLC analysis of tissue samples from dorsal striatum in HR, M16 and ICR mice was performed to measure tissue concentrations of DA, DOPAC, HVA, NE, 5HT and 5HIAA. Peptide concentrations for DA ($F(2,92) = 60.53$, $p < 0.001$), DOPAC ($F(2,92) = 34.34$, $p < 0.001$), HVA ($F(2,92) = 61.98$, $p < 0.001$), 5HT ($F(2,92) = 6.61$, $p < 0.01$) and 5HIAA ($F(2,92) = 7.37$, $p < 0.01$) were significantly higher in HR mice than in M16 or ICR mice. There were no differences in NE concentrations among the strains. 5HIAA concentrations were significantly higher in female compared to male mice across all three strains ($F(1,92) = 5.40$, $p < 0.05$). Female HR mice had lower, while M16 and ICR females had higher, DOPAC concentrations ($F(2,92) = 4.47$, $p < 0.05$) than their male counterparts. Data are presented as mean ± SEM.

decreased in the nucleus accumbens of ob/ob mice [29]. Moreover, obese rats are less motivated to respond for food reward in an operant conditioning paradigm and show decreased DA turnover in the NA [42]. Reduced dopaminergic signaling in these obese models is proposed to signify enhanced motivation for food intake whereby dopamine deficient animals seek food reward in an attempt to increase dopaminergic signaling, thus leading to obese phenotypes [5]. Alternatively, decreased dopamine turnover may occur as the result of persistent hyperphagia-induced dopamine release [42]. M16 mice are selected for increased growth and body mass at 3–6 weeks of age. During this developmental period, M16 mice display significant hyperphagia, which contributes to the obesity phenotype [23,43,44]. Thus, decreased DA turnover in M16 mice may be evidence for hyperphagia-induced neuroadaptation within central reward pathways. Although dopaminergic dysregulation is evident in obese M16 mice, the role of the dopaminergic system in the ontogeny of the obesity phenotype is not clear.

Several genes involved in the dopamine signaling pathway were differentially expressed among HR, M16, and ICR mouse strains in the dorsal striatum. For example, transcripts encoding the dopamine D1a and D2 receptor genes were down-regulated in both HR and M16 mice compared to ICR. Down-regulation of transcripts encoding the dopamine D1a receptor gene in the dorsal striatum of HR mice was accompanied by a down-regulation of transcripts encoding *Gnal* (adenylate cyclase-stimulating G-protein, alpha, *Golf*), the key G-protein involved in D1 receptor signal transduction, and *Adcy5* (adenlyate cyclase 5) was down-regulated in both HR and M16 mice. Transcripts encoding adenylate cyclase subtypes and activating polypeptides were also differentially expressed in the dorsal striatum of HR and M16 mice compared with ICR mice. These genes are involved in second-messenger signaling of G-protein coupled receptors, such as those described above. When gene expression in the dorsal striatum was analyzed separately by running condition, there was little difference in the transcripts that were differentially expressed between active and inactive male HR or M16 mice compared with ICR mice. However, M16 mice allowed to run for 6 days displayed down-regulation of *Gnal* compared to ICR mice. These results clearly show that dopaminergic signaling is different in HR and M16 mice compared with ICR controls, yet the exact function of these genes in dopaminergic signaling and interactions with other neurotransmitter systems in HR and M16 mice requires further study (see [45]).

Gene expression analyses within the nucleus accumbens identified several genes that may be involved in the neurological changes that occur within the dopaminergic system of animals bred for high rates of wheel running or increased body mass. For example, HR mice displayed increased expression of *Nr4a2* compared to both the ICR and M16 mice. Similarly, M16 mice showed increased *Nr4a2* expression compared to ICR mice, but only when given access to a running-wheel. *Nr4a2*, or *Nurr1*, is a key player in DA neuronal differentiation, development of the midbrain dopaminergic system, and DA neurotransmission and has been associated with locomotor activity, wheel running, and reward-mediated behaviors [46,47]. Thus, upregulation of *Nurr1* in the nucleus accumbens of HR mice compared with ICR controls may complement increased DA concentrations and physical activity in these animals. Moreover, upregulation of *Nurr1* in M16 mice, only when they had access to a running-wheel, may indicate that wheel running acts to increase dopamine neurotransmission in this strain, perhaps serving as a reinforcing stimulus.

**Table 3**
Differential gene expression in the dorsal striatum between HR and ICR male mice.

| Gene ID | | Fold change | Description |
|---|---|---|---|
| Gfap | + | 3.85 | Glial fibrillary acidic protein |
| Mapkll | + | 3.21 | Mitogen-activated protein kinase 11 |
| Adcyapl | + | 3.04 | Adenylate cyclase activating polypeptide 1 |
| Klc2 | + | 2.80 | Kinesin complex: microtubule motor activity |
| Tp53ill | + | 2.76 | Tumor protein p53 inducible protein 11 |
| Osbplla | + | 2.26 | Oxysterol binding protein-like 1A |
| Oprsl | + | 2.03 | Opioid receptor, sigma 1 |
| Npylr | + | 1.97 | Neuropeptide Y receptor Yl |
| Junb | + | 1.87 | JUN-B oncogene |
| Mapk8ip3 | + | 1.87 | Mitogen-activated protein kinase 8 interacting protein 3 |
| Mapkapk2 | + | 1.86 | MAP kinase-activated protein kinase 2 |
| Jundl | + | 1.83 | Jun proto-oncogene related gene dl |
| Adcy2 | + | 1.78 | Adenylate cyclase 2 |
| Aktlsl | + | 1.74 | AKT1 substrate 1 (proline-rich) |
| Snca | + | 1.63 | Synuclein, alpha |
| Jun | + | 1.62 | Jun oncogene |
| MapklO | + | 1.62 | Mitogen-activated protein kinase 10 |
| Adcy8 | + | 1.60 | Adenylate cyclase 8 |
| Oprl | + | 1.54 | Orphan receptor; opioid receptor-like 1 |
| Ucp2 | + | 1.53 | Uncoupling protein 2, mitochondrial |
| Drdla | – | 2.91 | Dopamine receptor D1A |
| Adcy5 | – | 2.70 | Adenylate cyclase 5 |
| Cdk5rl | – | 2.68 | Cyclin-dependent kinase 5, regulatory subunit 1 |
| Gnal | – | 2.66 | Adenylate cyclase-stimulating G alpha protein |
| Adra2c | – | 2.24 | Adrenergic receptor, alpha 2 c |
| Drd2 | – | 2.18 | Dopamine receptor 2 |
| Gnaq | – | 2.12 | Guanine nucleotide binding protein, alpha q polypeptide |
| Pccb | – | 1.96 | Propionyl Coenzyme A carboxylase, beta polypeptide |
| Akt2 | – | 1.96 | Thymoma viral proto-oncogene 2 |
| Atf4 | – | 1.82 | Activating transcription factor 4 |
| Fosb | – | 1.81 | FBJ osteosarcoma oncogene B |
| Akt3 | – | 1.74 | Thymoma viral proto-oncogene 3 |
| Klfl6 | – | 1.73 | Kruppel-like factor 16 |
| Htrld | – | 1.73 | 5-Hydroxytryptamine (serotonin) receptor ID |
| Adcyaplrl | – | 1.71 | Adenylate cyclase activating polypeptide 1 receptor 1 |
| Gria3 | – | 1.71 | Glutamate receptor, ionotropic, AMPA3 (alpha 3) |
| Oprkl | – | 1.71 | Opioid receptor, kappa 1 |
| Cdk5rapl | – | 1.67 | CDK5 regulatory subunit associated protein 1 |

The results described within this manuscript are consistent with existing data demonstrating that HR mice have dopaminergic dysfunction, resulting in hyperactivity not only in the running-wheel but also in the home cage [13,37,38]. Pharmacologic experiments have demonstrated that HR mice have altered sensitivity to the behavioral effects of dopaminergic drugs [13,14]. For instance, HR mice decrease while control mice increase wheel running in response to ritalin administration [14]. Likewise, HR mice decrease while control mice do not alter running-wheel activity in response to the dopamine reuptake inhibitors cocaine and GBR12909 [13]. Moreover, a recent study [48] examining dopamine receptor expression in inbred strains with innate differences in wheel running reported that D1 receptors and tyrosine hydroxylase, the rate-limiting enzyme for dopamine production, were significantly down-regulated in the nucleus accumbens and dorsal striatum of a high-running inbred strain of mice compared to a low-running inbred strain. These differences in gene expression were the result of genetic differences in the inbred strains, and

**Table 4**
Diffe rential gene expression in the D orsal Stri atum of H R and ICR m ale mice with and with out access to running wheels for 6 days.

| Runner | | | Non-runner | | |
|---|---|---|---|---|---|
| Gene ID | | Fold change | Gene ID | | Fold change |
| Gfap | + | 3.79 | Gfap | + | 3.91 |
| Mapkll | + | 3.29 | Klc2 | + | 3.33 |
| Adcyapl | + | 3.26 | Mapkll | + | 3.25 |
| Tp53ill | + | 2.74 | Adcyapl | + | 2.84 |
| Osbplla | + | 2.47 | Tp53ill | + | 2.77 |
| Klc2 | + | 2.35 | Junb | + | 2.09 |
| Nr4a2[a] | + | 2.18 | Oprsl | + | 2.08 |
| Npylr | + | 2.16 | Osbplla | + | 2.07 |
| Oprsl | + | 1.98 | Jundl | + | 2.06 |
| Adcy2 | + | 1.87 | Mapkapk2 | + | 2.05 |
| Mapk8ip3 | + | 1.83 | Mapk8ip3 | + | 1.91 |
| Snca | + | 1.75 | Oprsl | + | 1.80 |
| Aktlsl | + | 1.71 | Npylr | + | 1.80 |
| Mapkapk2 | + | 1.69 | Ucp2[a] | + | 1.78 |
| Junb | + | 1.68 | Aktlsl | + | 1.77 |
| Gfap | + | 1.64 | MapklO | + | 1.74 |
| Jundl | + | 1.62 | Jun | + | 1.72 |
| Adcy8 | + | 1.56 | Adcy2 | + | 1.68 |
| Jun | + | 1.53 | Adcy8 | + | 1.64 |
| MapklO | + | 1.51 | Oprl[a] | + | 1.63 |
| Drdla | – | 2.71 | Snca | + | 1.52 |
| Adcy5 | – | 2.50 | Gfap | + | 1.51 |
| Gnal | – | 2.36 | Gnaq[a] | – | 3.64 |
| Adra2c | – | 2.16 | Drdla | – | 3.13 |
| Drd2 | – | 2.12 | Adcy5 | – | 2.93 |
| Akt2[a] | – | 2.04 | Adra2c | – | 2.32 |
| Pccb | – | 1.93 | Drd2 | – | 2.25 |
| Atf4[a] | – | 1.89 | Pccb | – | 1.98 |
| Htrld | – | 1.77 | Oprkl | – | 1.92 |
| Klfl6 | – | 1.77 | Fosb | – | 1.88 |
| Pdyn[a] | – | 1.76 | Gnal | – | 1.85 |
| Fosb | – | 1.73 | Cdk5rapl | – | 1.78 |
| Adcyaplrl[a] | – | 1.64 | Klfl6 | – | 1.69 |
| Cdk5rapl | – | 1.57 | Htrld | – | 1.69 |
| Oprkl | – | 1.53 | | | |

[a] Indicates gene transcripts whose expression differs by running condition.

**Table 5**
Differential gene expression in the dorsal striatum between M16 and ICR male mice.

| Gene ID | | Fold change | Description |
|---|---|---|---|
| Gnaq | + | 3.25 | Guanine nucleotide binding protein, alpha q polypeptide |
| Adcy9 | + | 1.69 | Adenylate cyclase 9 |
| Mapkll | + | 1.65 | Mitogen-activated protein kinase 11 |
| Adcyapl | + | 1.58 | Adenylate cyclase activating polypeptide 1 |
| Drdla | – | 1.92 | Dopamine receptor D1A |
| Adcy5 | – | 1.91 | Adenylate cyclase 5 |
| Drd2 | | 1.80 | Dopamine receptor 2 |
| Htrld | – | 1.61 | 5-Hydroxytryptamine (serotonin) receptor ID |

**Table 6**
Differential gene expression in the dorsal striatum of M16 and ICR male mice with and without access to running wheels for 6 days.

| Runner | | | Non-runner | | |
|---|---|---|---|---|---|
| Gene ID | | Fold change | Gene ID | | Fold change |
| Gnaq[a] | + | 4.87 | Adcy5 | – | 1.76 |
| Drdla | – | 2.20 | Drd2 | – | 1.71 |
| Adcy5 | – | 2.06 | Drdla | – | 1.68 |
| Htrld[a] | – | 1.90 | | | |
| Drd2 | – | 1.89 | | | |
| Gnal[a] | – | 1.85 | | | |
| Ppplrlb[a] | – | 1.63 | | | |
| Adra2c[a] | – | 1.59 | | | |

[a] Indicates gene transcripts whose expression differs by running condition.

**Table 7**
Differential gene expression in the nucleus accumbens of male mice with and without access to running wheels for 6 days.

| Runner | | | Non-runner | | |
|---|---|---|---|---|---|
| Gene ID | Fold change | | Gene ID | | Fold change |
| HR vs. ICR | | | | | |
| Nr4a2 | + | 2.40 | Nr4a2 | + | 2.48 |
| Snca | + | 1.68 | Mapkl | + | 1.57 |
| Mapkll | + | 1.57 | MapklO | + | 1.53 |
| | | | Snca | + | 1.51 |
| | | | Mapk8ip3 | + | 1.50 |
| M16 vs. ICR | | | | | |
| Gnaq | + | 3.47 | Gnaq | + | 2.78 |
| Nr4a2 | + | 1.90 | Osbp | – | 2.30 |
| Osbp | – | 1.52 | | | |

running-wheel activity had no statistical effect on gene expression [48].

The HR behavioral, pharmacologic, and D1and D2 gene expression traits are reminiscent of traits characterizing the dopamine transporter knockout (DAT KO) mouse. The dopamine transporter, through its rapid uptake of DA, controls the temporal and spatial activity of synaptic DA. DAT KO mice are characterized by hyperlocomotion in novel environments and enhanced perseverative behaviors [49], hyperlocomotor activity that is attenuated by psychostimulants like methylphenidate and cocaine, and reduced expression of D1 and D2 receptors compared to wild type mice [50]. In contrast to HR mice, DAT KO mice exhibit low levels of striatum DA, but higher extracellular and slower clearance levels than wild type mice resulting in a hyperdopaminergic state [50,51]. In HR mice the perseverative exercise phenotype, elevated DA levels, and down-regulation of D1 and D2 receptors indicate a hyperdopaminergic phenotype as well. Since HR mice exhibit a paradoxical decrease in wheel running behavior following methylphenidate and cocaine [13,14] it is possible that HR mice are also characterized by dopamine transporter deficiency. Interestingly, a dopamine transporter binding QTL has been reported on MMU7: 46.2 cM [52] near a QTL detected for average and maximum wheel running speed on MMU7: 53.39 in a HR × C57BL/6J backcross [53].

Likewise, alterations in dopamine receptor expression and dopamine neurotransmission have been implicated in the etiology of obesity. Obese individuals have been shown to have decreased D2 receptor expression [3,4]. Obesity-prone rats have decreased receptor expression accompanied by decreased extracellular DA levels in the nucleus accumbens [5,41]. Although M16 mice did not show decreased tissue DA levels in the NA, they did display decreased DA turnover, revealing a deficiency in DA neurotransmission within this brain area. D1 receptors have been associated with palatable food intake and the motivation to acquire food-related reward [54–56]. The fact that transcripts encoding D1 receptors are down-regulated in M16 mice suggests that these mice may have a reduced sensitivity to food-related reward.

In summary, these data demonstrate significant differences in CNS dopamine concentrations and gene expression in mice selectively bred for extreme exercise or obesity-related phenotypes. HR mice demonstrated significantly elevated dopamine concentrations in the mesolimbic and nigrostriatal reward pathways. These increases in dopamine and its metabolites were accompanied by down-regulation of gene transcripts encoding dopamine receptors, corresponding G-proteins and second-messenger signaling molecules. Similarly, while M16 mice did not show increased dopamine concentrations within the CNS, they did demonstrate decreased dopamine turnover and similar down-regulation of transcripts encoding DA receptors and second-messenger signaling molecules compared with ICR controls. These data suggest that aberrant functioning of the dopaminergic system may underlie both excessive exercise and obesity-related phenotypes. Speculatively, we may hypothesize that DNA variation in genes controlling and/or regulating this system can act as substrate for diametric selection responses depending on the phenotype under selection. However, further evidence to support this must be based on validation using replicated selection lines in order to differentiate actual selection responses from effects caused by genetic drift. Nonetheless, our findings may inform clinical research by providing targets for pharmacologic interventions to treat obesity-related disorders and compulsive exercise or hyperactivity phenotypes that are often comorbid with disorders such as anorexia nervosa or attention deficit-hyperactivity disorder.

**Table 8**
Differential gene expression in the Nucleus Accumbens of female mice allowed access to running wheels for 6 days.

| HRvs.ICR | | | M16vs.ICR | | |
|---|---|---|---|---|---|
| Gene ID | Fold change | | Gene ID | | Fold change |
| Nr4a2 | + | 1.99 | Gnaq | + | 3.59 |
| Gfap | – | 1.57 | Nr4a2 | + | 1.75 |
| | | | Sdfr2 | + | 1.71 |
| | | | Osbp | – | 1.91 |

## Acknowledgements

This research was supported by NIDDK grant DK076050 (DP) and a pilot award from NIH Roadmap Grant P20RR020649 ("An Interdisciplinary Strategy for Obesity"). WFM was supported by an NIMH training grant T32MH076694. Phenotypes were collected using the Animal Metabolism Phenotyping core facility within UNC's Clinical Nutrition Research Center (funded by NIDDK grant DK056350).

## Appendix A. Supplementary data

Supplementary data associated with this article can be found, in the online version, at doi:10.1016/j.bbr.2010.02.016.

## References

[1] Arnsten AF. Fundamentals of attention-deficit/hyperactivity disorder: circuits and pathways. J Clin Psychiatry 2006;67(Suppl. 8):7–12.
[2] Blum K, Chen AL, Braverman ER, Comings DE, Chen TJ, Arcuri V, et al. Attention-deficit-hyperactivity disorder and reward deficiency syndrome. Neuropsychiatr Dis Treat 2008;4:893–918.
[3] Davis C, Levitan RD, Kaplan AS, Carter J, Reid C, Curtis C, et al. Reward sensitivity and the D2 dopamine receptor gene: a case-control study of binge eating disorder. Prog Neuropsychopharmacol Biol Psychiatry 2008;32:620–8.
[4] Davis CA, Levitan RD, Reid C, Carter JC, Kaplan AS, Patte KA, et al. Dopamine for "Wanting" and opioids for "Liking": a comparison of obese adults with and without binge eating. Obesity 2009;17(6):1220–5 (Silver Spring).
[5] Geiger BM, Behr GG, Frank LE, Caldera-Siu AD, Beinfeld MC, Kokkotou EG, et al. Evidence for defective mesolimbic dopamine exocytosis in obesity-prone rats. Faseb J 2008;22:2740–6.
[6] Gruber R, Joober R, Grizenko N, Leventhal BL, Cook Jr EH, Stein MA. Dopamine transporter genotype and stimulant side effect factors in youth diagnosed with attention-deficit/hyperactivity disorder. J Child Adolesc Psychopharmacol 2009;19:233–9.
[7] Xu X, Mill J, Sun B, Chen CK, Huang YS, Wu YY, et al. Association study of promoter polymorphisms at the dopamine transporter gene in attention deficit hyperactivity disorder. BMC Psychiatry 2009;9:3.
[8] Belke TW. Responding for sucrose and wheel-running reinforcement: effect of pre-running. Behav Processes 2006;71:1–7.
[9] Belke TW. Concurrent schedules of wheel-running reinforcement: choice between different durations of opportunity to run in rats. Learn Behav 2006;34:61–70.
[10] Belke TW, Christie-Fougere MM. Investigations of timing during the schedule and reinforcement intervals with wheel-running reinforcement. Behav Processes 2006;73:240–7.
[11] Lett BT, Grant VL, Byrne MJ, Koh MT. Pairings of a distinctive chamber with the aftereffect of wheel running produce conditioned place preference. Appetite 2000;34:87–94.

[12] Belke TW, Garland Jr T. A brief opportunity to run does not function as a reinforcer for mice selected for high daily wheel-running rates. J Exp Anal Behav 2007;88:199–213.
[13] Rhodes JS, Hosack GR, Girard I, Kelley AE, Mitchell GS, Garland Jr T. Differential sensitivity to acute administration of cocaine, GBR 12909, and fluoxetine in mice selectively bred for hyperactive wheel-running behavior. Psychopharmacology (Berl) 2001;158:120–31.
[14] Rhodes JS, Garland T. Differential sensitivity to acute administration of Ritalin, apomorphine, SCH 23390, but not raclopride in mice selectively bred for hyperactive wheel-running behavior. Psychopharmacology (Berl) 2003;167:242–50.
[15] Rhodes JS, Gammie SC, Garland Jr T. Neurobiology of mice selected for high voluntary wheel-running activity. Integrat Comp Biol 2005;45:438–55.
[16] Kaplan AS, Levitan RD, Yilmaz Z, Davis C, Tharmalingam S, Kennedy JL. A DRD4/BDNF gene-gene interaction associated with maximum BMI in women with bulimia nervosa. Int J Eat Disord 2008;41:22–8.
[17] Levitan RD, Masellis M, Basile VS, Lam RW, Kaplan AS, Davis C, et al. The dopamine-4 receptor gene associated with binge eating and weight gain in women with seasonal affective disorder: an evolutionary perspective. Biol Psychiatry 2004;56:665–9.
[18] Cagniard B, Balsam PD, Brunner D, Zhuang X. Mice with chronically elevated dopamine exhibit enhanced motivation, but not learning, for a food reward. Neuropsychopharmacology 2006;31:1362–70.
[19] Blum K, Braverman ER, Holder JM, Lubar JF, Monastra VJ, Miller D, et al. Reward deficiency syndrome: a biogenetic model for the diagnosis and treatment of impulsive, addictive, and compulsive behaviors. J Psychoactive Drugs 2000;32(Suppl. i–iv):1–112.
[20] Girard I, McAleer MW, Rhodes JS, Garland Jr T. Selection for high voluntary wheel-running increases speed and intermittency in house mice (Mus domesticus). J Exp Biol 2001;204:4311–20.
[21] Nehrenberg DL, Hua K, Estrada-Smith D, Garland Jr T, Pomp D. Voluntary exercise and its effects on body composition depend on genetic selection history. Obesity 2009;17(7):1402–9 (Silver Spring).
[22] Swallow JG, Koteja P, Carter PA, Garland Jr T. Food consumption and body composition in mice selected for high wheel-running activity. J Comp Physiol B 2001;171:651–9.
[23] Allan MF, Eisen EJ, Pomp D. The M16 mouse: an outbred animal model of early onset polygenic obesity and diabesity. Obes Res 2004;12:1397–407.
[24] Franklin A, Kao A, Tapscott S, Unis A. NeuroD homologue expression during cortical development in the human brain. J Child Neurol 2001;16:849–53.
[25] Kilts CD, Breese GR, Mailman RB. Simultaneous quantification of dopamine, 5-hydroxytryptamine and four metabolically related compounds by means of reversed-phase high-performance liquid chromatography with electrochemical detection. J Chromatogr 1981;225:347–57.
[26] Martin P, Ohno M, Southerland SB, Mailman RB, Suzuki K. Heterotypic sprouting of serotonergic forebrain fibers in the brindled mottled mutant mouse. Brain Res Dev Brain Res 1994;77:215–25.
[27] McCarthy DJ, Smyth GK. Testing significance relative to a fold-change threshold is a TREAT. Bioinformatics 2009;25:765–71.
[28] Patterson TA, Lobenhofer EK, Fulmer-Smentek SB, Collins PJ, Chu TM, Bao W, et al. Performance comparison of one-color and two-color platforms within the MicroArray Quality Control (MAQC) project. Nat Biotechnol 2006;24:1140–50.
[29] Fulton S, Pissios P, Manchon RP, Stiles L, Frank L, Pothos EN, et al. Leptin regulation of the mesoaccumbens dopamine pathway. Neuron 2006;51:811–22.
[30] Rhodes JS, Garland Jr T, Gammie SC. Patterns of brain activity associated with variation in voluntary wheel-running behavior. Behav Neurosci 2003;117:1243–56.
[31] Foley TE, Greenwood BN, Day HE, Koch LG, Britton SL, Fleshner M. Elevated central monoamine receptor mRNA in rats bred for high endurance capacity: implications for central fatigue. Behav Brain Res 2006;174:132–42.
[32] Foley TE, Fleshner M. Neuroplasticity of dopamine circuits after exercise: implications for central fatigue. Neuromol Med 2008;10:67–80.
[33] Wu N, Cepeda C, Zhuang X, Levine MS. Altered corticostriatal neurotransmission and modulation in dopamine transporter knock-down mice. J Neurophysiol 2007;98:423–32.
[34] Waters RP, Renner KJ, Pringle RB, Summers CH, Britton SL, Koch LG, et al. Selection for aerobic capacity affects corticosterone, monoamines and wheel-running activity. Physiol Behav 2008;93:1044–54.
[35] Hattori S, Naoi M, Nishino H. Striatal dopamine turnover during treadmill running in the rat: relation to the speed of running. Brain Res Bull 1994;35:41–9.
[36] Meeusen R, Smolders I, Sarre S, de Meirleir K, Keizer H, Serneels M, et al. Endurance training effects on neurotransmitter release in rat striatum: an in vivo microdialysis study. Acta Physiol Scand 1997;159:335–41.
[37] Malisch JL, Breuner CW, Gomes FR, Chappell MA, Garland Jr T. Circadian pattern of total and free corticosterone concentrations, corticosteroid-binding globulin, and physical activity in mice selectively bred for high voluntary wheel-running behavior. Gen Comp Endocrinol 2008;156:210–7.
[38] Malisch JL, Breuner CW, Kolb EM, Wada H, Hannon RM, Chappell MA, et al. Behavioral despair and home-cage activity in mice with chronically elevated baseline corticosterone concentrations. Behav Genet 2009;39:192–201.
[39] Swallow JG, Carter PA, Garland Jr T. Artificial selection for increased wheel-running behavior in house mice. Behav Genet 1998;28:227–37.
[40] Dishman RK. Brain monoamines, exercise, and behavioral stress: animal models. Med Sci Sports Exerc 1997;29:63–74.
[41] Geiger BM, Haburcak M, Avena NM, Moyer MC, Hoebel BG, Pothos EN. Deficits of mesolimbic dopamine neurotransmission in rat dietary obesity. Neuroscience 2009;159:1193–9.
[42] Davis JF, Tracy AL, Schurdak JD, Tschop MH, Lipton JW, Clegg DJ, et al. Exposure to elevated levels of dietary fat attenuates psychostimulant reward and mesolimbic dopamine turnover in the rat. Behav Neurosci 2008;122:1257–63.
[43] Eisen EJ, Leatherwood JM. Adipose cellularity and body composition in polygenic obese mice as influenced by preweaning nutrition. J Nutr 1978;108:1652–62.
[44] Eisen EJ, Leatherwood JM. Effect of postweaning feed restriction on adipose cellularity and body compositon in polygenic obese mice. J Nutr 1978;108:1663–72.
[45] Keeney BK, Raichlen DA, Meek TH, Wijeratne RS, Middleton KM, Gerdeman GL, et al. Differential response to a selective cannabinoid receptor antagonist (SR141716: rimonabant) in female mice from lines selectively bred for high voluntary wheel-running behaviour. Behav Pharmacol 2008;19:812–20.
[46] Rojas P, Joodmardi E, Hong Y, Perlmann T, Ogren SO. Adult mice with reduced Nurr1 expression: an animal model for schizophrenia. Mol Psychiatry 2007;12:756–66.
[47] Werme M, Hermanson E, Carmine A, Buervenich S, Zetterstrom RH, Thoren P, et al. Decreased ethanol preference and wheel running in Nurr1-deficient mice. Eur J Neurosci 2003;17:2418–24.
[48] Knab AM, Bowen RS, Hamilton AT, Gulledge AA, Lightfoot JT. Altered dopaminergic profiles: implications for the regulation of voluntary physical activity. Behav Brain Res 2009;204(1):147–52.
[49] Gainetdinov RR, Jones SR, Fumagalli F, Wightman RM, Caron MG. Re-evaluation of the role of the dopamine transporter in dopamine system homeostasis. Brain Res Brain Res Rev 1998;26:148–53.
[50] Giros B, Jaber M, Jones SR, Wightman RM, Caron MG. Hyperlocomotion and indifference to cocaine and amphetamine in mice lacking the dopamine transporter. Nature 1996;379:606–12.
[51] Jones SR, Gainetdinov RR, Jaber M, Giros B, Wightman RM, Caron MG. Profound neuronal plasticity in response to inactivation of the dopamine transporter. Proc Natl Acad Sci USA 1998;95:4029–34.
[52] Jones SR, Gainetdinov RR, Hu XT, Cooper DC, Wightman RM, White FJ, et al. Loss of autoreceptor functions in mice lacking the dopamine transporter. Nat Neurosci 1999;2:649–55.
[53] Nehrenberg DL, Wang S, Hannon RM, Garland Jr T, Pomp D. QTL underlying voluntary exercise in mice: interactions with the "mini muscle" locus and sex. J Hered 2010;101:42–53.
[54] Katz JL, Kopajtic TA, Terry P. Effects of dopamine D1-like receptor agonists on food-maintained operant behavior in rats. Behav Pharmacol 2006;17:303–9.
[55] MacDonald AF, Billington CJ, Levine AS. Alterations in food intake by opioid and dopamine signaling pathways between the ventral tegmental area and the shell of the nucleus accumbens. Brain Res 2004;1018:78–85.
[56] Terry P, Katz JL. Differential antagonism of the effects of dopamine D1-receptor agonists on feeding behavior in the rat. Psychopharmacology (Berl) 1992;109:403–9.
[57] Bronikowski AM, Rhodes JS, Garland Jr T, Prolla TA, Awad TA, Gammie SC. The evolution of gene expression in mouse hippocampus in response to selective breeding for increased locomotor activity. Evolution 2004;58:2079–86.

**Supplementary Table 1. Gene transcripts evaluated for differential expression among HR, ICR and M16 mice.**

| Target ID | Accession | Symbol | Definition |
|---|---|---|---|
| scl026414.2_6-S | NM_009158 | Mapk10 | Mus musculus mitogen activated protein kinase 10 (Mapk10), mRNA. |
| scl0001307.1_2-S | NM_016961.2 | Mapk9 | Mus musculus mitogen activated protein kinase 9 (Mapk9), transcript variant 2, mRNA. |
| ri\|1200011E13\|R000009K | AK004704 | Pdcl | phosducin-like |
| scl0071720.1_33-S | NM_027881.1 | Osbpl3 | Mus musculus oxysterol binding protein-like 3 (Osbpl3), mRNA. |
| scl50915.17_55-S | NM_011951 | Mapk14 | Mus musculus mitogen activated protein kinase 14 (Mapk14), mRNA. |
| scl0224129.19_263-S | XM_358801.1 | Adcy5 | Mus musculus adenylate cyclase 5 (Adcy5), mRNA. |
| scl0014580.2_305-S | NM_010277.1 | Gfap | Mus musculus glial fibrillary acidic protein (Gfap), mRNA. |
| scl018166.3_27-S | NM_010934.1 | Npy1r | Mus musculus neuropeptide Y receptor Y1 (Npy1r), mRNA. |
| scl0003403.1_22-S | NM_011643.1 | Trpc1 | Mus musculus transient receptor potential cation channel, subfamily C, member 1 (Trpc1), mF |
| scl0066596.2_43-S | NM_025652.1 | Gtf3a | Mus musculus general transcription factor III A (Gtf3a), mRNA. |
| scl45744.1.427_89-S | NM_021712.1 | Slc18a3 | Mus musculus solute carrier family 18 (vesicular monoamine), member 3 (Slc18a3), mRNA. |
| GI_6679121-S | NM_008731.1 | Npy2r | Mus musculus neuropeptide Y receptor Y2 (Npy2r), mRNA. |
| scl030957.1_28-S | NM_013931.1 | Mapk8ip3 | Mus musculus mitogen-activated protein kinase 8 interacting protein 3 (Mapk8ip3), mRNA. |
| scl19785.7_63-S | NM_031373.2 | Ogfr | Mus musculus opioid growth factor receptor (Ogfr), mRNA. |
| scl24813.3_604-S | NM_008309.2 | Htr1d | Mus musculus 5-hydroxytryptamine (serotonin) receptor 1D (Htr1d), mRNA. |
| scl0001427.1_15-S | NM_144828.1 | Ppp1r1b | Mus musculus protein phosphatase 1, regulatory (inhibitor) subunit 1B (Ppp1r1b), mRNA. |
| scl0002395.1_4-S | AK030714.1 | | Mus musculus RIKEN full-length enriched library, pro-opiomelanocortin-alpha, full insert seq |
| scl0013488.2_233-S | NM_010076.1 | Drd1a | Mus musculus dopamine receptor D1A (Drd1a), mRNA. |
| scl18671.5_48-S | NM_018863.2 | Pdyn | Mus musculus prodynorphin (Pdyn), mRNA. |
| scl31374.5.1_14-S | NM_007527.2 | Bax | Mus musculus Bcl2-associated X protein (Bax), mRNA. |
| scl016443.4_14-S | NM_010587.1 | Itsn1 | intersectin 1 (SH3 domain protein 1A) |
| scl43956.3_488-S | NM_010076 | Drd1a | Mus musculus dopamine receptor D1A (Drd1a), mRNA. |
| scl18476.16.14_21-S | NM_025876.1 | Cdk5rap1 | Mus musculus CDK5 regulatory subunit associated protein 1 (Cdk5rap1), mRNA. |
| scl35445.15.1_13-S | NM_025835.1 | Pccb | Mus musculus propionyl Coenzyme A carboxylase, beta polypeptide (Pccb), mRNA. |
| scl53349.15_2-S | XM_148904 | Osbp | oxysterol binding protein |
| scl0011516.2_115-S | NM_009625.2 | Adcyap1 | Mus musculus adenylate cyclase activating polypeptide 1 (Adcyap1), mRNA. |
| scl34746.2_217-S | NM_016708 | Npy5r | Mus musculus neuropeptide Y receptor Y5 (Npy5r), mRNA. |
| scl0002989.1_42-S | NM_016886.1 | Gria3 | Mus musculus glutamate receptor, ionotropic, AMPA3 (alpha 3) (Gria3), mRNA. |
| scl053623.15_103-S | NM_016886.1 | Gria3 | Mus musculus glutamate receptor, ionotropic, AMPA3 (alpha 3) (Gria3), mRNA. |
| scl47132.18.1_100-S | NM_009623.1 | Adcy8 | Mus musculus adenylate cyclase 8 (Adcy8), mRNA. |
| scl32891.21_547-S | NM_007434 | Akt2 | Mus musculus thymoma viral proto-oncogene 2 (Akt2), mRNA. |
| scl0026417.1_62-S | NM_011952.1 | Mapk3 | Mus musculus mitogen activated protein kinase 3 (Mapk3), mRNA. |
| scl0014682.1_7-S | NM_008139.2 | Gnaq | Mus musculus guanine nucleotide binding protein, alpha q polypeptide (Gnaq), mRNA. |
| scl18924.1.2532_104-S | NM_008036 | Fosb | Mus musculus FBJ osteosarcoma oncogene B (Fosb), mRNA. |
| scl000466.1_7-S | NM_008451.1 | Klc2 | Mus musculus kinesin light chain 2 (Klc2), mRNA. |
| scl54377.16.1_8-S | NM_172778.1 | Maob | Mus musculus monoamine oxidase B (Maob), mRNA. |
| scl021804.11_211-S | NM_009365.2 | Tgfb1i1 | Mus musculus transforming growth factor beta 1 induced transcript 1 (Tgfb1i1), mRNA. |
| scl35598.8_175-S | NM_015806.2 | Mapk6 | Mus musculus mitogen-activated protein kinase 6 (Mapk6), mRNA. |
| scl014680.2_22-S | NM_010307 | Gnal | guanine nucleotide binding protein (G protein), alpha |
| scl22689.16.1_37-S | NM_009146 | Sdfr2 | Mus musculus stromal cell derived factor receptor 2 (Sdfr2), mRNA. |
| scl0002267.1_458-S | NM_020573.1 | Osbpl1a | Mus musculus oxysterol binding protein-like 1A (Osbpl1a), mRNA. |
| scl0011517.1_49-S | NM_007407.2 | Adcyap1r1 | Mus musculus adenylate cyclase activating polypeptide 1 receptor 1 (Adcyap1r1), mRNA. |
| GI_6678046-S | NM_009221.1 | Snca | Mus musculus synuclein, alpha (Snca), mRNA. |
| scl39495.10_537-S | NM_010277 | Gfap | Mus musculus glial fibrillary acidic protein (Gfap), mRNA. |
| scl35495.10.1_8-S | NM_011643.1 | Trpc1 | Mus musculus transient receptor potential cation channel, subfamily C, member 1 (Trpc1), mF |
| scl019094.1_245-S | NM_011161.4 | Mapk11 | Mus musculus mitogen-activated protein kinase 11 (Mapk11), mRNA. |
| scl46858.9.1_36-S | NM_013871.2 | Mapk12 | Mus musculus mitogen-activated protein kinase 12 (Mapk12), mRNA. |
| scl0002696.1_5-S | NM_011014.1 | Oprs1 | Mus musculus opioid receptor, sigma 1 (Oprs1), mRNA. |
| scl38880.29_102-S | NM_011179 | Psap | Mus musculus prosaposin (Psap), mRNA. |
| scl26804.8_290-S | NM_007668.2 | Cdk5 | Mus musculus cyclin-dependent kinase 5 (Cdk5), mRNA. |
| scl53486.15_226-S | NM_008451 | Klc2 | Mus musculus kinesin light chain 2 (Klc2), mRNA. |
| scl067605.5_228-S | NM_026270.1 | Akt1s1 | Mus musculus AKT1 substrate 1 (proline-rich) (Akt1s1), mRNA. |
| scl41621.13_164-S | NM_207692.1 | Mapk9 | Mus musculus mitogen activated protein kinase 9 (Mapk9), transcript variant 2, mRNA. |
| scl0378430.1_272-S | NM_194064.1 | Nanos2 | Mus musculus nanos homolog 2 (Drosophila) (Nanos2), mRNA. |
| scl37728.2_209-S | NM_078477 | Klf16 | Mus musculus Kruppel-like factor 16 (Klf16), mRNA. |
| scl36981.8.1_23-S | NM_010077.1 | Drd2 | Mus musculus dopamine receptor 2 (Drd2), mRNA. |
| scl47732.2_4-S | XM_139474.1 | Atf4 | Mus musculus activating transcription factor 4 (Atf4), mRNA. |
| scl52769.3.1_151-S | NM_009073 | Rom1 | Mus musculus rod outer segment membrane protein 1 (Rom1), mRNA. |
| scl16317.12_198-S | NM_008551.1 | Mapkapk2 | Mus musculus MAP kinase-activated protein kinase 2 (Mapkapk2), mRNA. |
| scl00100273.2_58-S | NM_133885.1 | Osbpl9 | Mus musculus oxysterol binding protein-like 9 (Osbpl9), mRNA. |
| scl0002227.1_9-S | NM_010307 | Gnal | guanine nucleotide binding protein (G protein), alpha |
| scl48681.7.1_1-S | XM_147265.1 | Comt | Mus musculus catechol-O-methyltransferase (Comt), mRNA. |
| scl0002534.1_775-S | NM_011161.4 | Mapk11 | Mus musculus mitogen-activated protein kinase 11 (Mapk11), mRNA. |
| scl026413.2_16-S | NM_011949.2 | Mapk1 | Mus musculus mitogen activated protein kinase 1 (Mapk1), mRNA. |
| scl20407.30.36_15-S | NM_011941 | Mapkbp1 | Mus musculus mitogen activated protein kinase binding protein 1 (Mapkbp1), mRNA. |

**Supplementary Table 1 (cont). Gene transcripts evaluated for differential expression among HR, ICR and M16 mice.**

| Target ID | Accession | Symbol | Definition |
|---|---|---|---|
| scl00100273.2_58-S | NM_133885.1 | Osbpl9 | Mus musculus oxysterol binding protein-like 9 (Osbpl9), mRNA. |
| scl0002227.1_9-S | NM_010307 | Gnal | guanine nucleotide binding protein (G protein), alpha |
| scl48681.7.1_1-S | XM_147265.1 | Comt | Mus musculus catechol-O-methyltransferase (Comt), mRNA. |
| scl0002534.1_775-S | NM_011161.4 | Mapk11 | Mus musculus mitogen-activated protein kinase 11 (Mapk11), mRNA. |
| scl026413.2_16-S | NM_011949.2 | Mapk1 | Mus musculus mitogen activated protein kinase 1 (Mapk1), mRNA. |
| scl20407.30.36_15-S | NM_011941 | Mapkbp1 | Mus musculus mitogen activated protein kinase binding protein 1 (Mapkbp1), mRNA. |
| scl30062.4.1_1-S | NM_023456.2 | Npy | Mus musculus neuropeptide Y (Npy), mRNA. |
| GI_31982683-S | NM_021921.2 | Mapk8ip2 | Mus musculus mitogen-activated protein kinase 8 interacting protein 2 (Mapk8ip2), mRNA. |
| GI_83582785-A | NM_001037723.1 | Adcy7 | Mus musculus adenylate cyclase 7 (Adcy7), transcript variant 2, mRNA. |
| scl00035.1_45-S | NM_011671.2 | Ucp2 | Mus musculus uncoupling protein 2, mitochondrial (Ucp2), mRNA. |
| scl18186.3.1_175-S | NM_011011.1 | Oprk1 | Mus musculus opioid receptor, kappa 1 (Oprk1), mRNA. |
| scl43784.25.1_156-S | NM_153534.1 | Adcy2 | Mus musculus adenylate cyclase 2 (Adcy2), mRNA. |
| scl0001776.1_145-S | NM_011949.2 | Mapk1 | Mus musculus mitogen activated protein kinase 1 (Mapk1), mRNA. |
| scl0277414.7_122-S | XM_203859 | Tp53i11 | Mus musculus tumor protein p53 inducible protein 11 (Tp53i11), mRNA. |
| scl48815.9.1_11-S | XM_148699.3 | Crebbp | Mus musculus CREB binding protein (Crebbp), mRNA. |
| scl54967.10.1218_2-S | NM_016886.1 | Gria3 | Mus musculus glutamate receptor, ionotropic, AMPA3 (alpha 3) (Gria3), mRNA. |
| scl33714.1_27-S | NM_010592.3 | Jund1 | Mus musculus Jun proto-oncogene related gene d1 (Jund1), mRNA. |
| scl45735.13_394-S | NM_016700 | Mapk8 | Mus musculus mitogen activated protein kinase 8 (Mapk8), mRNA. |
| scl35980.21.1_18-S | NM_175481.2 | Grik4 | Mus musculus glutamate receptor, ionotropic, kainate 4 (Grik4), mRNA. |
| scl1664.1.1_301-S | NM_007407 | Adcyap1r1 | Mus musculus adenylate cyclase activating polypeptide 1 receptor 1 (Adcyap1r1), mRNA. |
| scl31608.7.1_161-S | NM_181593.2 | Itpkc | Mus musculus inositol 1,4,5-trisphosphate 3-kinase C (Itpkc), mRNA. |
| scl0014285.1_257-S | | Fosr | |
| scl52314.6.1_5-S | NM_007452.1 | Prdx3 | Mus musculus peroxiredoxin 3 (Prdx3), mRNA. |
| scl24094.1_31-S | NM_010591.1 | Jun | Mus musculus Jun oncogene (Jun), mRNA. |
| scl33597.11_333-S | NM_008854 | Prkaca | Mus musculus protein kinase, cAMP dependent, catalytic, alpha (Prkaca), mRNA. |
| scl0012846.1_253-S | XM_147265.1 | Comt | Mus musculus catechol-O-methyltransferase (Comt), mRNA. |
| scl0001894.1_46-S | XM_147265.1 | Comt | Mus musculus catechol-O-methyltransferase (Comt), mRNA. |
| scl018391.1_236-S | NM_011014.1 | Oprs1 | Mus musculus opioid receptor, sigma 1 (Oprs1), mRNA. |
| scl45526.26.1_78-S | NM_080435.1 | Adcy4 | Mus musculus adenylate cyclase 4 (Adcy4), mRNA. |
| scl0003256.1_3-S | NM_025876.1 | Cdk5rap1 | Mus musculus CDK5 regulatory subunit associated protein 1 (Cdk5rap1), mRNA. |
| scl23999.29_549-S | NM_133885 | Osbpl9 | Mus musculus oxysterol binding protein-like 9 (Osbpl9), mRNA. |
| scl41169.1_6-S | NM_009871.2 | Cdk5r1 | cyclin-dependent kinase 5, regulatory subunit 1 (p35) |
| scl53314.1_457-S | NM_008139 | Gnaq | Mus musculus guanine nucleotide binding protein, alpha q polypeptide (Gnaq), mRNA. |
| scl47616.12_239-S | NM_021921 | Mapk8ip2 | Mus musculus mitogen-activated protein kinase 8 interacting protein 2 (Mapk8ip2), mRNA. |
| scl44430.1.474_5-S | NM_008308.2 | Htr1a | Mus musculus 5-hydroxytryptamine (serotonin) receptor 1A (Htr1a), mRNA. |
| scl21036.31.1_8-S | NM_177345.2 | Mapkap1 | Mus musculus mitogen-activated protein kinase associated protein 1 (Mapkap1), mRNA. |
| scl39113.8_92-S | NM_010511.1 | Ifngr1 | interferon gamma receptor 1 |
| scl0011652.2_199-S | NM_007434.2 | Akt2 | Mus musculus thymoma viral proto-oncogene 2 (Akt2), mRNA. |
| scl15142.1.1_162-S | NM_010307 | Gnal | guanine nucleotide binding protein (G protein), alpha |
| scl074309.1_115-S | NM_152818.1 | Osbp2 | Mus musculus oxysterol binding protein 2 (Osbp2), mRNA. |
| scl0228983.14_82-S | NM_144500.1 | Osbpl2 | Mus musculus oxysterol binding protein-like 2 (Osbpl2), mRNA. |
| scl015980.8_163-S | NM_008338.2 | Ifngr2 | Mus musculus interferon gamma receptor 2 (Ifngr2), mRNA. |
| scl00104252.2_200-S | NM_026772.1 | Cdc42ep2 | Mus musculus CDC42 effector protein (Rho GTPase binding) 2 (Cdc42ep2), mRNA. |
| scl48812.11_88-S | NM_009624.1 | Adcy9 | Mus musculus adenylate cyclase 9 (Adcy9), mRNA. |
| scl099031.19_30-S | NM_145525 | Osbpl6 | Mus musculus oxysterol binding protein-like 6 (Osbpl6), mRNA. |
| scl0002479.1_2-S | NM_013871.2 | Mapk12 | Mus musculus mitogen-activated protein kinase 12 (Mapk12), mRNA. |
| scl0001471.1_1-S | NM_207692.1 | Mapk9 | Mus musculus mitogen activated protein kinase 9 (Mapk9), transcript variant 2, mRNA. |
| scl0018227.2_224-S | NM_013613.1 | Nr4a2 | Mus musculus nuclear receptor subfamily 4, group A, member 2 (Nr4a2), mRNA. |
| scl15870.13_49-S | NM_011785.2 | Akt3 | Mus musculus thymoma viral proto-oncogene 3 (Akt3), mRNA. |
| scl00227743.1_265-S | NM_177345.2 | Mapkap1 | Mus musculus mitogen-activated protein kinase associated protein 1 (Mapkap1), mRNA. |
| scl018227.1_24-S | NM_013613 | Nr4a2 | Mus musculus nuclear receptor subfamily 4, group A, member 2 (Nr4a2), mRNA. |
| scl17784.1.1_200-S | NM_009872.1 | Cdk5r2 | Mus musculus cyclin-dependent kinase 5, regulatory subunit 2 (p39) (Cdk5r2), mRNA. |
| scl0026419.2_93-S | NM_016700.2 | Mapk8 | Mus musculus mitogen activated protein kinase 8 (Mapk8), mRNA. |
| scl27874.1.190_60-S | NM_013503.1 | Drd5 | Mus musculus dopamine receptor 5 (Drd5), mRNA. |
| scl026417.10_0-S | NM_011952.1 | Mapk3 | Mus musculus mitogen activated protein kinase 3 (Mapk3), mRNA. |
| scl0064291.1_176-S | NM_020573.1 | Osbpl1a | Mus musculus oxysterol binding protein-like 1A (Osbpl1a), mRNA. |
| scl8260.1.1_298-S | NM_016886 | Gria3 | Mus musculus glutamate receptor, ionotropic, AMPA3 (alpha 3) (Gria3), mRNA. |
| scl018389.7_4-S | NM_011012.2 | Oprl | |
| scl0099031.1_295-S | NM_145525.1 | Osbpl6 | Mus musculus oxysterol binding protein-like 6 (Osbpl6), mRNA. |
| scl48870.1_132-S | NM_010587 | Itsn1 | intersectin 1 (SH3 domain protein 1A) |
| scl18987.13.1_0-S | NM_011162.2 | Mapk8ip | Mus musculus mitogen activated protein kinase 8 interacting protein (Mapk8ip), mRNA. |
| scl43434.22.1_35-S | NM_138305.2 | Adcy3 | Mus musculus adenylate cyclase 3 (Adcy3), mRNA. |
| scl016477.1_58-S | NM_008416.1 | Junb | Mus musculus Jun-B oncogene (Junb), mRNA. |
| scl45926.20.1_29-S | NM_144844.1 | Pcca | Mus musculus propionyl-Coenzyme A carboxylase, alpha polypeptide (Pcca), mRNA. |
| scl39662.12.1_73-S | NM_030248.1 | Cdk5rap3 | Mus musculus CDK5 regulatory subunit associated protein 3 (Cdk5rap3), mRNA. |
| scl51269.7_133-S | NM_172632.1 | Mapk4 | Mus musculus mitogen-activated protein kinase 4 (Mapk4), mRNA. |
| scl30448.26_191-S | NM_024289 | Osbpl5 | Mus musculus oxysterol binding protein-like 5 (Osbpl5), mRNA. |
| scl000618.1_71-S | NM_010308 | Gnao | Mus musculus guanine nucleotide binding protein, alpha o (Gnao), mRNA. |
| scl0019047.1_2-S | NM_013636.2 | Ppp1cc | Mus musculus protein phosphatase 1, catalytic subunit, gamma isoform (Ppp1cc), mRNA. |
| scl41339.16.1_19-S | NM_145429.1 | Arrb2 | Mus musculus arrestin, beta 2 (Arrb2), mRNA. |
| scl27902.1_282-S | NM_007418.2 | Adra2c | Mus musculus adrenergic receptor, alpha 2c (Adra2c), mRNA. |